Research Report

Surface Labeling with Adhesion Protein FimH Improves Binding of Immunotherapeutic Agent *Salmonella* Ty21a to the Bladder Epithelium

Maroeska J. Burggraaf[a,1], Lisette Waanders[a,1], Mariska Verlaan[b], Janneke Maaskant[a],
Diane Houben[c], Joen Luirink[d], Wilbert Bitter[a,c], Coen Kuijl[a,2] and Carla F.M. Molthoff[b,2,*]

[a]*Department of Medical Microbiology and Infection Control, Amsterdam University Medical Center (AUMC), Location VU Medical Center (VUMC), Amsterdam, The Netherlands*
[b]*Department of Radiology & Nuclear Medicine, Amsterdam University Medical Center (AUMC), Location VU Medical Center (VUMC), Amsterdam, The Netherlands*
[c]*Section Molecular Microbiology, AIMMS, Vrije Universiteit, Amsterdam, The Netherlands*
[d]*Abera bioscience AB, Solna, Sweden*

Abstract.

BACKGROUND: Bladder cancer is the ninth most common cancer in men. 70% of these tumors are classified as non-muscle invasive bladder cancer and those patients receive 6 intravesical instillations with *Mycobacterium bovis* BCG after transurethral resection. However, 30% of patients show recurrences after treatment and experience severe side effects that often lead to therapy discontinuation. Recently, another vaccine strain, *Salmonella enterica typhi* Ty21a, demonstrated promising antitumor activity *in vivo*. Here we focus on increasing bacterial retention in the bladder in order to reduce the number of instillations required and improve antitumor activity.

OBJECTIVE: To increase the binding of Ty21a to the bladder wall by surface labeling of the bacteria with adhesion protein FimH and to study its effect in a bladder cancer mouse model.

METHODS: Binding of Ty21a with surface-labeled FimH to the bladder wall was analyzed *in vitro* and *in vivo*. The antitumor effect of a single instillation of Ty21a+FimH in treatment was determined in a survival experiment.

RESULTS: FimH-labeled Ty21a showed significant ($p < 0.0001$) improved binding to mouse and human cell lines *in vitro*. Furthermore, FimH labeled bacteria showed ∼5x more binding to the bladder than controls *in vivo*. Enhanced binding to the bladder via FimH labeling induced a modest improvement in median but not in overall mice survival.

CONCLUSIONS: FimH labeling of Ty21a significantly improved binding to bladder tumor cells *in vitro* and the bladder wall *in vivo*. The improved binding leads to a modest increase in median survival in a single bladder cancer mouse study.

Keywords: *Salmonella enterica*, Ty21a typhoid vaccine, immunotherapy, bladder cancer, FimH protein, *E. coli*

---

[1]Shared first authors.

[2]Shared senior authorship.

*Correspondence to: Dr. C.F.M. Molthoff, PhD, associate professor, Department of Radiology & Nuclear Medicine, Amsterdam University Medical Center (AUMC), location VU University Med-

ical Center (VUMC), Amsterdam, The Netherlands. Tel.: +31 20 444 9291; Fax: +31 20 444 9121; E-mail: cfm.molthoff@amsterdamumc.nl.

ABBREVIATIONS

BCG   *Mycobacterium bovis* Bacillus Calmette-Guérin
TURB   transurethral resection of the bladder
NMIBC   non-muscle invasive bladder cancer
RD1   region of difference 1
Ty21a   *Salmonella enterica typhi* Ty21a
UPEC   uropathogenic *Escherichia coli*
BLI   bioluminescence imaging

INTRODUCTION

Bladder cancer is the ninth most common cancer worldwide and the incidence in men is three times higher than in women [3]. On the other hand, women often show higher stages of cancer at the moment of diagnosis with a concomitant worse prognosis. 70% of the bladder cancers are non-muscle invasive (NMIBC) and are treated by transurethral resection of the bladder (TURB) followed by instillation of the bladder with chemotherapy or immunotherapy to reduce tumor recurrence [4].

Current immunotherapy consists of live *Mycobacterium bovis* Bacillus Calmette-Guerin (BCG), a bacterial vaccine strain well known for its use against tuberculosis in humans. Already since the 1980's BCG is known for its antitumor activity and has been used effectively in bladder cancer treatment [5]. Meta-analysis has shown that treatment with BCG is superior to chemotherapeutic Mitomycin C treatment with less recurrences [6]. However, even from those patients with the best prognosis, still approximately 30% may show recurrence of the tumor or are unable to complete the therapeutic regimen due to severe local and systemic side effects [7].

Recently, *Salmonella enterica typhi* Ty21a (Ty21a) has been shown to exert good potential as antitumor agent in mice [8]. To test the efficacy in humans, a phase I clinical trial has started that investigates Ty21a treatment in NMIBC (Identifier: NCT034212 36). Ty21a is an attenuated vaccine strain used against typhoid fever. In an orthotopic bladder cancer mouse model it was shown that already after one instillation, Ty21a could reduce tumor growth and enhance survival, whereas BCG required four treatments to reach equal effects[9]. Furthermore, experiments showing that Ty21a cannot survive in human PBMC cells from healthy donors, in human cell lines *in vitro* nor in a 3D-bladder tissue *ex vivo* model, suggest a favorable safety profile for Ty21a [8].

To investigate whether Ty21a in bladder cancer therapy can be further optimized, the SpyCatcher/ SpyTag system was used. The SpyTag is a short peptide that covalently binds to the SpyCatcher peptide [10]. We use the SpyCatcher/SpyTag technology combined with a modified autotransporter protein that was recently developed by van den Berg van Saparoea et al. [11]. In this system an autotransporter, the hemoglobin protease of *E. coli* (Hbp), lacking the protease activity and carrying a SpyTag, is heterologously expressed in Ty21a cells. This modified Hbp autotransporter is efficiently secreted to the cell surface and allows the covalent attachment of SpyCatcher-labelled proteins to the surface exposed SpyTag peptide sequence [12]. Virtually any target protein that its fused to SpyCatcher can then be efficiently coupled to the SpyTag. This leads to many possibilities for Ty21a treatment optimization while maintaining the Ty21a vaccine safety profile.

We hypothesized that immunotherapeutic efficacy could be improved by enhanced binding of Ty21a to the bladder wall. For BCG immunotherapy binding to the bladder wall has been shown to be important [13] and we hypothesized that the same could hold true for Ty21a treatment. To improve bladder wall binding, the strategy of uropathogenic *E. coli* (UPEC) was used. In this, pathogen binding to the bladder epithelium is mediated through Type I pili present on the bacterial cell surface [14]. Type I pili bind host cells through the FimH adhesin at the tip of the pilus. The adhesion domain of FimH binds mannosylated proteins on the cell surface of urothelial cells, *e.g.* uroplakin-Ia [1, 2]. FimH is required for binding of UPEC to the bladder wall [15, 16] and thereby important for virulence [17]. We use FimH as an adhesion protein to promote bacterial retention in the bladder.

In this study, we confirm the suitability of the SpyCatcher/SpyTag system to decorate Ty21a with the adhesion domain of FimH. It was shown that the FimH adhesion properties are maintained after coupling to Ty21a *in vitro* with T24, MB49 and Hela cells and *in vivo* with mouse bladders. Furthermore, antitumor activity of Ty21a with and without FimH have been compared in an orthotopic bladder cancer mouse model. The results showed that distinct increased adhesion can be achieved through FimH labeling, but the effect on bladder cancer treatment was limited *in vivo*.

MATERIAL AND METHODS

Mice and tumor cell instillation

C57BL/6 mice (female, 4–6 week old, for intravesical treatment experiments mice obtained from VU University Amsterdam, the Netherlands. For the KRAS and BLI analysis mice were obtained from Charles River, Wilmington, USA) were intravesically instilled with MB49-luc cells as described previously [18]. Briefly, at day 0 mice were anesthetized with 2% isoflurane/oxygen anesthetics (0.4 L/min). Thereafter, mice were catheterized and bladders were rinsed 3 times with PBS. Then the bladder wall was scratched carefully with a 24G blunted needle. Next, 3×10^3 MB49-luc cells were instilled in the bladder and incubated for 2 h. Mice were provided with standard food and water (ad libitum) under conditions described previously. All animal experiments were performed according to the criteria and guidelines of European Community Council Directive 2010/63/EU for laboratory animal care and the Dutch Law on animal experimentation. The experimental protocols (510-RNG19-44; 510-RNG-18-31; 510-RNG19-47A1) were approved by the local committee on animal experimentation of the VU University Amsterdam, The Netherlands (approval number AVD114002016510 / 0510-RNG19-47).

Cells and cell line identity

Murine MB49-luc cells stably expressing luciferase were kindly provided by prof.dr. T. Wurdinger (Amsterdam UMC, location VUmc, Amsterdam, The Netherlands). Cells were cultured in DMEM (Lonza, Verviers, Belgium), supplemented with 10% fetal calf serum (FCS) and 1% penicillin/streptomycin (Gibco Life Technologies, Grand Island, USA). Cells were authenticated by STR analysis (QIAGEN, Hilden, Germany). Luciferase expression was regularly checked by limited dilution methodology for high expressers (BLI, see below).

T24 cells (American Type Culture Collection HTB-4™) were cultured in RPMI1640 with 10% fetal calf serum (FCS; Gibco Life Technologies, Grand Island, USA). HeLa cells were kindly provided by prof. dr. D. Holden (Imperial College London, London, United Kingdom) and were cultured in DMEM with 10% fetal calf serum (FCS; Gibco Life Technologies, Grand Island, USA). RAW264.7 cells (American Type Culture Collection) were cultured in RPMI1640 with Glutamax-1 (Gibco Life Technologies, Grand Island, USA) supplemented with 10% FCS (Gibco Life Technologies, Grand Island, USA). All cells were cultured at 37°C with 5% CO_2. All cell lines were tested negative for mycoplasma (date last tested: 08/14/2020).

Bioluminescence imaging (BLI)

Mice were anesthetized 2% isoflurane/oxygen anesthetics (0.4 L/min) and abdominal hair was removed. 150 μl D-luciferin (Gold Biotechnology, St. Louis, USA) was subcutaneously injected in the neck region. After 18 minutes, mice BLI signals and X-ray were imaged using the *In-Vivo* Xtreme imager (Bruker, Leiderdorp, the Netherlands) and analyzed by using Bruker Molecular Imaging Software (version 7.5.2.22464).

Bacterial strains

Mycobacterium bovis BCG Tice was cultured in 7H9 liquid medium supplemented with Middlebrook ADC (Difco, BD Biosciences, Franklin Lanes, NJ USA) and 0.05% Tween-80 (Sigma, St. Louis, USA) at 37°C.

S. typhi Ty21a (Mutaflor, Germany) and *E. coli* Top10F' were cultured in LB medium supplemented with 0.2% glucose and, when appropriate, 30 μg/mL chloramphenicol at 37°C and shaking at 200 rpm. For competitive binding experiments LB medium was supplemented with 0.2% glucose and 0.001% galactose. *E. coli* BL-21 were grown in LB supplemented with 50 μM L-rhamnose, 100 μg/ml ampicillin and 30 ug/ml chloramphenicol at 30°C, 200 rpm.

DNA extraction from bladders

Bladders were homogenized with a pestle in TEN buffer (10 mM Tris-HCl, 1 mM EDTA, 100 mM NaCl in aquadest) and incubated overnight at 50°C with 1% SDS and 0.1 mg/ml Proteinase K. DNA was extracted by adding 0.8 volumes phenol/chloroform/isoamyl alcohol (25:24:1), followed by centrifugation. Then, 0.6 volumes isopropanol and NaAc (final conc. 0.3 M) were added to the aqueous phase and incubated for 1 hour at 4°C. After centrifugation, supernatant was removed and the pellet was washed with 70% ethanol. The pellet was dried at RT, dissolved in TE-1 buffer at 65°C for 15 minutes. As control samples, genomic DNA was extracted from RAW and MB49-luc cells in similar fashion.

KRAS analysis

A fragment spanning the first exon of KRAS was amplified with primer set KRAS_1_Fw (CTTTA-CAAGCGCACGCAGAC) and KRAS_1_Rv (AGGT-TACTCTGTACATCTGTAGTCA) by using Phusion polymerase (Thermo Scientific, Rockford, USA). Resulting bands were extracted from a 1% agarose gel with the GeneJET gel extraction kit (Thermo Scientific, Rockford, USA) and sent for sequencing by Macrogen Europe (Amsterdam, the Netherlands) with primer KRAS_1_Fw or KRAS_1_Rv. Sequence reads were analyzed by determining the location of the $G > A$ mutation and use 5 up and downstream A and G bases to calculate the average peak area of these bases on a wild type sequence read. This average peak area was used to determine the expected peak area at the mutation site for A and G. The measured peak area at the location of the $G > A$ mutation site is divided by either the expected A or G area, resulting in 2 values for the $G > A$ mutation: $A \div A(\text{expected}) = \text{mutation frequency}$ and $1\text{-}G \div G(\text{expected}) = \text{mutation frequency}$. The average of these two values is the fraction of $KRAS^{G34A}$ positive DNA. Analysis was performed using computing environment R (R foundation) [19]. Script is provided in Supplemental Data 1 and 2.

Plasmid construction

pET22-pelB-FimH-Spycatcher-his was created by inserting the following *pelB-**fimH**-HA* fragment coding for the adhesion domain of FimH, amino acids 22–180 in bold, ordered from Integrated DNA Technologies, Coralville, USA) in pET22b-*spycatcher-his* vector by In-Fusion cloning (ClonTech, Mountainview, USA).

ATGAAATACCTGCTGCCGACCGCTGCTGCT GGTCTGCTGCTCCTCGCTGCCCAGCCGGCGA TGGCC**TTTGCATGTAAGACGGCTAATGGCA CGGCAATTCCAATCGGGGGGGGGTAGTGCA AATGTGTATGTGAATCTTGCGCCCGCTGT TAATGTGGGACAAAATTTAGTAGTGGATTT GTCCACTCAGATTTTCTGTCACAATGATTA TCCAGAAACTATCACCGACTATGTGACTCT GCAACGCGGGGCCGCGTATGGCGGAGTAT TAAGCTCCTTTAGCGGAACGGTAAAATATA ACGGCTCGTCATACCCATTCCCTACAACTT CTGAGACTCCTCGCGTCGTTTACAATTCC CGCACTGATAAGCCGTGGCCAGTGGCACT TTACCTGACCCCAGTTTCCAGTGCTGGTG GAGTTGCTATTAAAGCCGGTTCATTGATTG**

CCGTTTTGATTTTACGCCAAACAAACAACT ATAACAGTGACGACTTCCAATTCGTGTGGA ACATCTATGCCAACAACGATGTTGTGGTCC CAACAGGC*AGCGGCGGA*TATCCCTACGATGT ACCGGATTACGCTGGATCCGGGGGGTACCGGC.

mScarlet was amplified from template plasmid *pET11A-mScarlet* (Abera Bioscience, Stockholm, Sweden) with primers pEH3-Scarlet-Fw (GAACAC ATCTCTGGATCGAACTTTAAGAAGGAGATATA CATAATGGTGAGCAAG) and pEH3-Scarlet-Rv (GTAAAACGACGGCCAGTGCTACTTGTACAG CTCGTCCATGC) by phusion polymerase (Thermo Scientific, Rockford, USA). *neonGreen* was amplified from *pet22b-Neongreen-SpC-His* (Abera Bioscience, Stockholm, Sweden) with primers Hbp-NG-Fw (GAACACATCTCTGGATCGAAGAAGGAGA TATACATATGGTAAGTAAAG) and Hbp-NG-Rv (GTAAAACGACGGCCAGTGCTACCTTGTACA GCTCGTCCATGC. The resulting amplicons were inserted in *pEH3-HbpD(d1)SpyTag* (Abera Bioscience, Stockholm, Sweden) by restriction with EcoRI (NEB, Ipswich, USA) followed by Gibson assembly, creating vectors *pEH3-HbpD(d1)SpyTag-mScarlet* and *pEH3-HbpD(d1)SpyTag-neonGreen*. Both vectors harbor the SpyTag at the N-terminus of Hbp.

E. coli BL-21 were transformed with *pET22b-pelB-FimH-spycatcher-his* by standard heat-shock protocol.

S. typhi Ty21a were washed with 10% glycerol and electroporated with *pEH3-HbpD(d1)SpyTag-mScarlet* and *pEH3-HbpD(d1)SpyTag-neonGreen*.

Isolation FimH-SpyCatcher

FimH-SpyCatcher was isolated from the periplasmic fraction of *E. coli* BL-21 expressing *pET22b-pelB-FimH-spycatcher-his*. At $OD_{600} = 0.3$, bacteria were incubated for 2 hours with 400 μM isopropyl β-D-1-thiogalactopyranoside (IPTG) to induce expression. Bacteria were harvested and washed with 20 mM tris(hydroxymethyl)aminomethaan (Tris) (pH 8). Pellets were resuspended in 20 mM Tris (pH 8) with 2 mg/ml lysozyme and proteinase inhibitor mix (Roche). Sphaeroplast formation was stabilized by adding 10 mM $MgCl_2$ at a conversion of 90%. Sphaeroplasts were removed by centrifugation and the soluble FimH-SpyCatcher containing supernatant was dialyzed to remove EDTA. FimH-SpyCatcher was subsequently isolated by His-purification according to manufacturer's protocol (TALON Superflow, GE Healthcare, Chicago,

USA). The eluate was dialyzed to remove imidazole and the concentration was determined by a BCA assay according to manufacturer's protocol (Thermo Scientific, Rockford, USA).

FimH labeling

Labeling was performed using the SpyTag-Spy Catcher system [12, 20]. Hemoglobin protease (Hbp) was used as a carrier to enable surface exposure of the SpyTag [21]. Overnight pre-culture of bacteria was diluted to $OD_{600} = 0.05$ and grown to $OD_{600} = 0.3$ when Hbp-SpyTag expression was induced with 1 mM IPTG and incubated for 3h at $37°C$. To prevent binding of excessive unbound FimH to unlabeled bacteria in competition experiments, non-labeled Ty21a bacteria were labeled with recombinant SpyCatcher-maltose binding protein (MPB). Then, bacteria were harvested and washed with PBS. Bacteria were resuspended in PBS and incubated with $40 \mu g$ FimH-HA-SpyCatcher overnight at $4°C$. Bacteria were washed once with PBS before use and resuspended in Krebs-Ringer-HEPES buffer (KRP) supplemented with 1.85 mM calcium and 1.3 mM Mg.

Binding assays

MB49-luc (160.000 cells/well), T24 (160.000 cells/well) and HeLa (60.000 cells/well) were incubated with an equivalent of $OD_{600} = 0.05$ FimH labeled or unlabeled bacteria for 1 h and then washed with KRP with 1.85 mM calcium and 1.3 mM Mg. Cells were fixated with 4% PFA (Sigma, St. Louis, USA) for 30 minutes. HeLa cells were permeabilized with 0.1% Triton-X100 (Sigma, St. Louis, USA) and incubated 15 minutes on ice. After washing with PBS, cells were stained with Hoechst (1:2000 in PBS, Invitrogen, Carlsbad, USA) and Oregon Green™ 488 Phalloidin (1:200 in PBS, Invitrogen, Carlsbad, USA).

For competitive binding assays, FimH labeled and MBP labeled bacteria were mixed in a 1:1 ratio in PBS with 1 mM calcium and 1 mM Mg. Bacteria were washed with and diluted in PBS. Mice were intravesically instilled with $100 \mu l$ bacterial mix (17.4×10^5 CFU) for 1 hour according to the procedure for intravesical instillation described above. After sacrificing the mice, bladders were fixated with 4% PFA for 1.5 hours and resected from the mice. Bladders were cut open, 3 times washed with PBS and incubated in Hoechst (1:500 in PBS, Invitrogen, Carlsbad, USA) for 1 hour. Then, bladders were put under a coverslip

with Vectashield antifade mounting medium (H-1000, Vector Laboratories, Peterborough, UK) and sealed with cover sealant (Biotium, Fremont, USA).

Microscopical analysis

Widefield microscopic images of *in vitro* experiments were taken with Olympus IX83 inverted microscope analyzed with cell image analysis software (Cellprofiler version 3.1.5). The fluorescent intensities of Ty21a mScarlet signal were determined when associated with GFP-actin defined HeLa cells. The mScarlet signals (Z) depicted in the graphs are normalized by the formula $Z=(x-min)/(max-min)$, in which x is the raw mScarlet signal, min is the lowest mScarlet signal and max is the highest mScarlet signal. Ratios of labeled/unlabeled bacteria were corrected for the input ratios.

Whole mounted bladders of the *in vivo* competitive binding experiment were imaged with confocal microscopy (Nikon A1 plus). Pixels that showed a fluorescent signal of mScarlet or NeonGreen were counted in each Z-stack of every image. Pixel counts were accumulated for all images per mouse and corrected for the input CFU (as counted by CFU plating). Then, the ratio NeonGreen/mScarlet pixels per mouse was calculated.

Immunoblot analysis

Bacteria were washed with PBS and resuspended in SDS sample buffer (50 mM Tris-HCl, 100 mM dithiothreitol (DTT), 2% sodium dodecyl sulphate (SDS), 5 mM ehtylenediaminetetraacetic acid (EDTA), 10% glycerol). Samples were separated by SDS PAGE and transferred to a nitrocellulose filter by Western blotting. Blots were blocked with 5% milk in PBS and stained with anti-HA (HA 1.11) and goat-anti-mouse IgG peroxidase-labelled antibodies (American Qualex Antibodies, San Clemente, USA). Imaging was performed with electro-chemiluminescence Western Blotting Detection Reagent (Amersham Bioscience, Amersham, UK).

Survival experiment

Mice were anesthetized and catheterized and instilled with MB49-luc on day 0 as described above and after rinsing bladders, mice were instilled with $100 \mu l$ Ty21a coupled to FimH, Ty21a or PBS on day 5, aiming for 3×10^7 CFU Ty21a (actual CFU without FimH: 3.7×10^7, with FimH: 2.4×10^7)

and incubated for 1h. Input CFU was determined based on study by Domingos-Pereira et al. 2016 [8]. BLI was measured at day 8, only mice that showed positive BLI signal (at least 1.5x higher intensity than the background signal) continued in the experiment. Body weight was monitored 3 times per week and overall well-being was evaluated every day. Sacrificed mice that did not show a bladder tumor upon resection were not included in Kaplan-Meier analysis.

Statistical analysis

Ty21a binding with or without FimH *in vitro* was analyzed with an unpaired T test. Fold change binding in competition experiment with FimH labeled bacteria was analyzed with a one-sample *t*-test. The median survival was analyzed by Wilcoxon-signed rank test.

RESULTS

Labeling of Ty21a with FimH to improve bladder binding

We hypothesized that *S. enterica typhi* Ty21a immunotherapy can be improved by enhancing adhesion of the bacteria to the bladder wall, as adhesion is the first important and essential step in BCG immunotherapy [13]. To examine this, bacteria were labelled with FimH by using Hbp autotransporter SpyCatcher/SpyTag system [11]. Using this method, the FimH protein is not expressed constitutively, but the bacterial cell surface is only decorated extensively with the adhesion domain of FimH before instillation. In the system described by van den Berg van Saparoea et al. the Hbp protein is abundantly expressed on the bacterial cell surface and modified to expose a spytag at the distal end [11]. Subsequently, these bacteria are incubated with recombinant SpyCatcher-FimH carrying an HA-tag. The binding of SpyCatcher to SpyTag results in a spontaneous intramolecular isopeptide bond and thus the covalent attachment of FimH to the surface of Ty21a. The formation of the FimH-SpyCatcher:Hbp-SpyTag complex was analyzed by immunoblot analysis using HA antibodies (Fig. 1A). Upon incubation with the SpyCatcher-HA-FimH protein the appearance of a protein conjugate with the predicted molecular weight of ∼140kDa could be observed, indicating that the conjugation was successful (Fig. 1A).

To determine whether FimH could improve binding *in vitro*, FimH-labeled Ty21a bacteria were incubated with the human epithelial cell line HeLa. FimH-labeled Ty21a showed significantly more binding to HeLa cells as compared to unlabeled bacteria ($p < 0.0001$) (Fig. 1B). Subsequently, we tested the binding of FimH-labeled Ty21a bacteria to a human and a murine bladder cancer cell line, T24 and MB49, respectively. Again, a highly improved binding was observed (Fig. 1B), indicating that the binding characteristics of Ty21a have been significantly improved by FimH surface labeling.

Next, the effect of FimH labeling on binding of bacteria to the bladder wall was studied *in vivo* in C57BL/6 mice. In a competition assay, bladders were instilled with a mixture of FimH labeled (expressing NeonGreen) and MBP labeled (expressing mScarlet) Ty21a bacteria. MBP was used to prevent binding of excess FimH to the mScarlet Ty21a control by binding to the SpyTag present in Hbp. Microscopical analysis showed that bacteria were not evenly distributed over the tissue, but appeared in patches (Fig. 1C). A minimum of 4 of these patches per mouse ($n = 7$) were analyzed for binding of FimH labeled and unlabeled bacteria by fluorescent confocal microscopy (Fig. 1C). FimH-labeled bacteria showed 4.9 times more binding than unlabeled bacteria ($p = 0.005$). This is in agreement with the *in vitro* obtained results. These experiments showed an improved binding of *S. enterica typhi* Ty21a bacteria to the bladder wall upon decoration with the adhesion domain FimH.

Read-out analysis of tumor growth

To investigate the effect of Ty21a coupled to FimH in a bladder cancer mouse model, a reliable method is needed to determine tumor take and preferably tumor size as well. Tumor growth can be measured *in vivo* by bioluminescence imaging (BLI) and *ex vivo* by assessing bladder weight. However, although monitoring tumor growth over time *in vivo* can be instrumental, it is not clear yet whether BLI can be used as an exact measure of tumor growth. Bladder weight on the other hand might be affected by influx of healthy stromal cells and immune cells into the tumor. To determine which method is most reliable to measure tumor growth, we compared BLI signals, tumor weight and DNA compositions of untreated bladders at several days after tumor cell instillation. For this, 15 mice were instilled with MB49 tumor
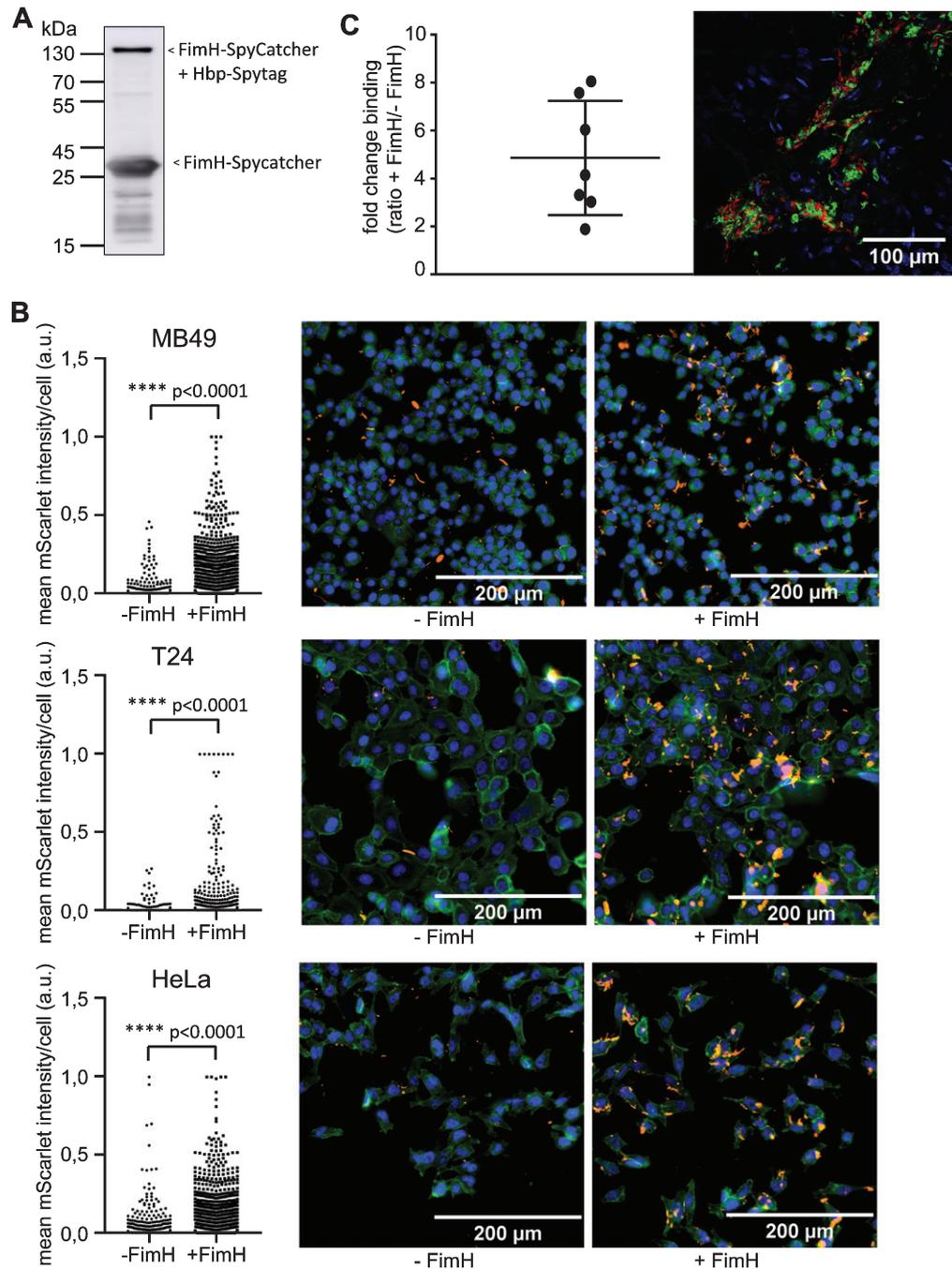
Fig. 1. Analysis of bacterial binding upon surface labeling of *S. enterica typhi* Ty21a with FimH. (A) Immunoblot showing FimH-SpyCatcher (∼30 kDa) and Hbp-SpyTag labeled with FimH-SpyCatcher (∼140 kDa) as present in labeled Ty21a. Bacterial pellet representing 0.1 OD units (OD_{600}) was loaded and polyclonal antiserum directed against the HA tag was used. (B) Fluorescent microscopy images of MB49, T24 and HeLa cells incubated for 1 h with FimH labeled (+FimH) or unlabeled (-FimH) Ty21a (red). After fixation, actin was stained in green and nuclei in blue. Graph shows mean mScarlet intensity/cell for unlabeled Ty21a (-FimH) and FimH labeled Ty21a (+FimH). Intensities were corrected for input CFU. Statistical analysis: unpaired *T*-test. (C) Mice were instilled with a mix of FimH labeled Ty21a (neonGreen) and MBP labeled Ty21a (mScarlet). Confocal microscopy z-stack images of a minimum of 3 patches per mouse (*n* = 7) were scored for the presence of neonGreen and mScarlet bacteria. Representative single slide of z-stack is shown. Fold change binding depicts the ratio of neonGreen/mScarlet bacteria after correction for input CFU. Statistical analysis: one sample *T*-test.
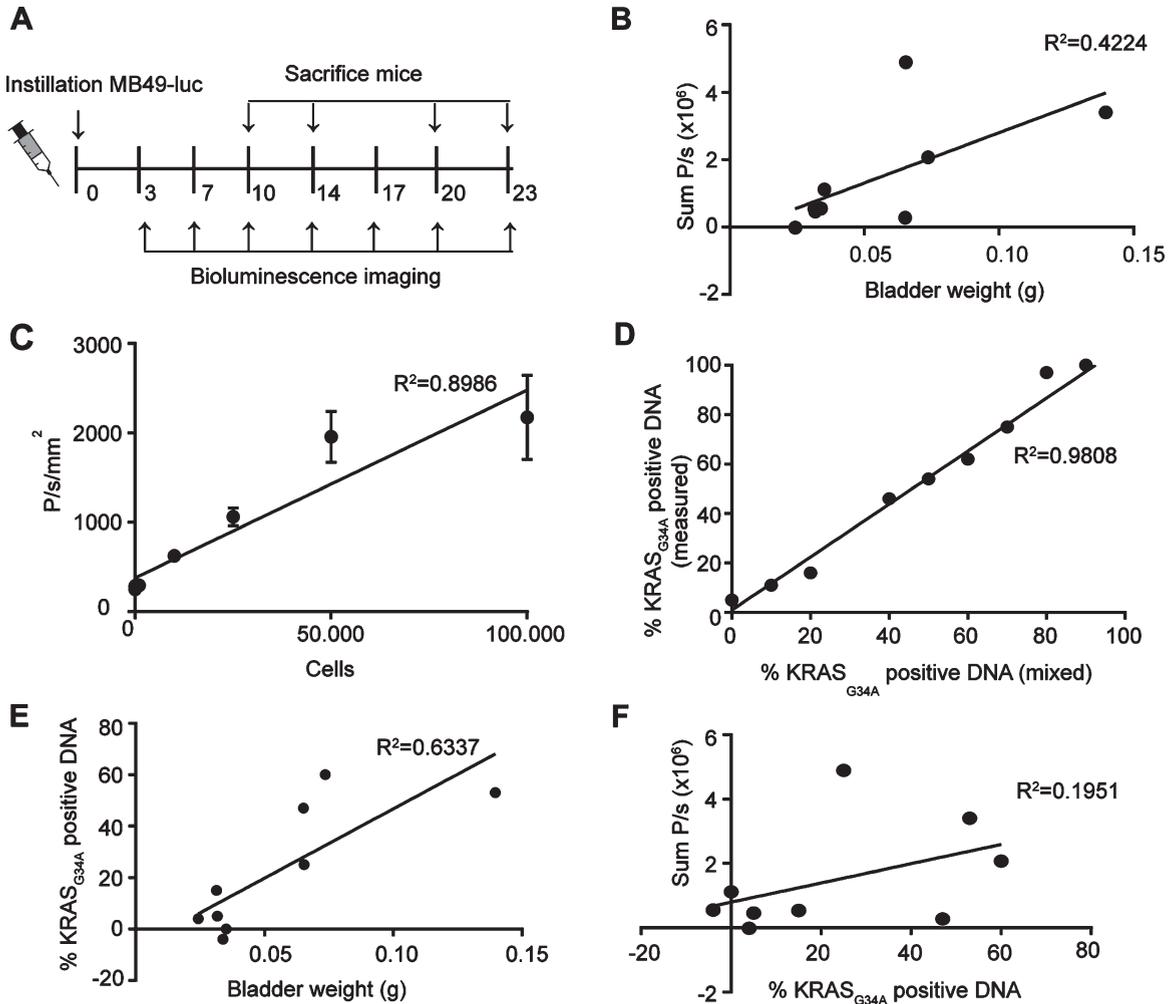
Fig. 2. Comparison BLI and bladder weight for analysis of tumor growth. (A) Schematic overview of experimental set-up. (B) Correlation plot of BLI signal over bladder weight ($n = 9$). (C) *In vitro* analysis of BLI signal of MB49-luc cells. (D) Correlation plot of $KRAS_{G34A}$ positive DNA as measured by sequencing over $KRAS_{G34A}$ positive DNA as mixed before sequencing. Genomic DNA was isolated from RAW cells ($KRAS_{G34}$) and MB49-luc ($KRAS_{A34}$) and mixed in depicted proportions. (E) Correlation plot of percentage of $KRAS_{G34A}$ positive cells as determined by sequence analysis over bladder weight ($n = 9$). (F) Correlation plot of BLI signal and percentage of $KRAS_{G34A}$ positive DNA ($n = 9$). (B,E,F) Only bladders with tumors were taken into account.

cells expressing luciferase, and BLI was measured at day 3, 7, 10, 14, 17, 20 and 23 after instillation. To compare different tumor sizes with BLI measurements, 3–5 mice were sacrificed at days 10, 14, 20 and 23 and bladders were isolated for further analysis (Fig. 2A).

After tumor cell instillation 9 out of 15 mice had developed a tumor at the day of sacrifice as based on macroscopic analysis. Only bladders with a tumor were taken into account for further analysis. Tumor-bearing bladders did not show a significant correlation between the BLI signal and the bladder weight ($R^2 = 0.4224$, $p = 0.0581$)(Fig. 2B, see

Supplemental Data 3 for all bladders). This might seem remarkable, since BLI signal shows a linear relationship with the number of MB49-luc cells *in vitro* ($R^2 = 0.8986$, $p = 0.0003$) (Fig. 2C). Although the low amount of tumor bearing bladders make it difficult to find a significant correlation, the low correlation might also be due to the contribution of non-tumor cells to the total tumor weight *in vivo*.

To determine the percentage of MB49 cells from the total amount of cells in the tumor, we analyzed the DNA of the bladders with tumors for the presence of a specific mutation in KRAS. This mutation is present in MB49-luc cells but not in wild type

Fig. 3. Survival experiment bladder cancer mouse model with Ty21a and FimH treatment. (A) Schematic overview of experimental set-up. Mice received $3*10^3$ MB49-luc cells at day 0 and were treated at day 5. Mice that developed tumors at day 8 according to BLI Ty21a+FimH ($n = 10$), Ty21a ($n = 15$) and PBS ($n = 7$) were included for survival analysis. (B) Kaplan-Meier curve showing survival of mice treated with Ty21a+FimH, Ty21A and PBS. (C) Median survival of different treatment groups. Mice which died and showed a bladder tumor upon macroscopic analysis are presented as filled circles. Mice which showed no sign of a bladder tumor upon macroscopic analysis are considered 'cured'. These are presented as open circles.

cells of C57BL/6 mice [22]. Control samples with a known percentage of MB49-luc DNA showed a linear relationship between the percentage of DNA with the $KRAS_{G34A}$ mutation and the percentage of DNA with or without the $KRAS_{G34A}$, as calculated from the relative peak area for the mutated base in the sanger sequence trace ($R^2 = 0.9808$, $p < 0.0001$) (Fig. 2D).

Genomic DNA of the bladders was isolated and the percentage of $KRAS_{G34A}$ positive DNA present was determined. A significant correlation was found between bladder weight and the percentage of $KRAS_{G34A}$ positive DNA ($R^2 = 0.6337$, $p = 0.0103$) (Fig. 2E). In contrast, no correlation was found for the percentage of $KRAS_{G34A}$ positive DNA with the BLI signal ($R^2 = 0.1951$, $p = 0.2339$) (Fig. 2F), suggesting that the BLI signal is not an accurate measure of tumor size.

In conclusion, bladder weight is a reliable measure for the amount of tumor cells and thus to measure anti-tumor activity but not feasible in a longitudinal study since bladder weight can only be assessed *ex vivo*. In contrast, BLI is less reliable but can give an indication of tumor take and initial tumor growth *in vivo*. For our following *in vivo* experiment, we therefore resorted to BLI to solely assess tumor take.

Survival experiment using Ty21a labeled with FimH

S. enterica typhi Ty21a coupled to FimH showed significant improved binding *in vitro* and *in vivo*. We continued this research by investigating whether improved binding would also improve bladder cancer therapy. Therefore, a well-designed single mice survival experiment with the orthotopic bladder cancer mouse model was conducted. Mice were treated 5 days after tumor instillation with either Ty21a+FimH, Ty21a or PBS (Fig. 3A). At day 8 after instillation tumor take was verified with BLI to determine which mice were to be included in the *in vivo* study. Day 8 was chosen based on previous experiments showing tumor growth from day 7 [18]. Overall survival curves did not show a significant effect of Ty21a, either coupled to FimH or not, as compared to the PBS treated control mice (Fig. 3B). The highest median survival is seen in the TY21a+FimH treated group (42,5 days), followed by Ty21a (39 days) and PBS (33 days) (Fig. 3C). These results indicate that, although *S. enterica typhi* Ty21a cells do have a modest positive effect on the median survival in the bladder cancer mouse model, this effect is not improved upon enhanced bladder wall attachment (Ty21a+FimH:Ty21a $p = 0.2031$).

DISCUSSION

Resection of the tumor followed by intravesical BCG immunotherapy is the current standard treatment for non-muscle invasive bladder cancer in human. However, even with BCG therapy still ~30% recurrences occur [7, 23]. Furthermore, about 65% of patients report local or systemic side effects with BCG treatment. In 8% of these cases, treatment was discontinued and only 16% of the patients received all scheduled maintenance therapies [24, 25]. The majority of patients did not adhere to the 3 year treatment and did therefore not receive all scheduled instillations[24, 26]. Therefore, improving intravesical bladder cancer therapy is necessary.

In a previous study, it was shown that *S. enterica typhi* Ty21a is significantly better as compared to BCG in the treatment regimen in bladder cancer in mice [8, 9]. Currently, a phase I clinical trial has started with Ty21a in NMIBC (NCT03421236). The classical effective treatment regimen to study BCG immunotherapy in orthotopic bladder cancer mouse models consists of 4 treatments at one week intervals, starting 1 day after tumor instillation. Interestingly, it was shown that Ty21a required only one instillation, whereas BCG requires 4 instillations to induce partial antitumor activity [8]. With the single instillation in case of Ty21a several advantages can be envisioned, such as to greatly reduce the number of anesthetizing and catheterization rounds. If the latter also holds true for the clinical situation, it would also greatly reduce the discomfort for patients which often leads to discontinued treatment. Therefore, in this study we tested whether Ty21a treatment could be further improved by increasing the binding of Ty21a to the bladder epithelium by decorating the bacteria with adhesion protein FimH.

An important advantage of Ty21a compared to BCG is its safety profile. Ty21a is an attenuated strain of *S. enterica typhi* not able to survive within cells, but harboring the capacity to evoke immune responses [9, 27]. Another advantage of Ty21a is the lack of disseminating capacity to other organs like spleen and lymph nodes in the mouse after intravesical instillation. Furthermore, Ty21a does not survive in human cells nor in an 3D-bladder-tissue *ex vivo* assay, suggesting an improved safety profile as compared to BCG [8].

With respect to cystitis, the main adverse local side-effect of BCG therapy in approximately 35% of clinical cases [24], it was reported that *E. coli* FimH enhances the ability to traffic from the bladder to deeper tissues and initiate cystitis [28]. Theoretically, labeling Ty21a with FimH could therefore enable dissemination. To prevent conceivable dissemination of FimH-labeled-Ty21a, Ty21a was not recombinantly modified to express type I pili. In our approach we labeled extracellularly with purified adhesion domain of FimH via the SpyCatcher/SpyTag system. This means that the pilus is not intact. Furthermore, FimH is not genetically encoded in Ty21a, hence daughter cells will not harbor FimH on their cell surface and the possibility of dissemination facilitated through FimH will be restricted.

First, the study aimed to improve binding of Ty21a to the bladder epithelium by decorating Ty21a with FimH. FimH has been shown before to be crucial for binding to the urothelium in *E. coli* [28]. Here we showed that labeling Ty21a with FimH increased binding to bladder cancer cell lines T24 and MB49 but also epithelial cell line HeLa. Moreover, competition experiments with FimH labeled and MBP labeled Ty21a showed 4.9 times more binding to the bladder for FimH labeled bacteria. Importantly, the FimH adhesion domain was able to increase binding not only when part of the type I pili complex in *E. coli*, but also when linked to the cell surface protein Hbp on Ty21a.

We also assessed the accuracy of BLI for measuring tumor growth *in vivo*. A previous study demonstrated that BLI signals reach a plateau over time while tumor size increases, as was confirmed by high resolution ultrasound imaging [18]. Here, we looked in more detail to the correlations between BLI and bladder weight. Analysis of the tumor composition, *e.g.* the percentage of MB49-luc tumor cells present, showed that the percentage of tumor DNA correlated with the bladder weight. This indicates that, as expected, MB49-luc cells are the main cell type present in the tumor. However, no significant correlation was found for the BLI signal and the bladder weight. Thus, bladder weight is a more accurate measure of tumor growth than BLI, but can obviously not be assessed *in vivo*.

The discrepancy between BLI signal and tumor size can be explained by several factors. First, the chemical reaction of luciferase with luciferin requires oxygen and ATP. By photoacoustic imaging it was shown that the amount of oxygen available in the bladder tumor decreases over time [18]. Secondly, the BLI signal might be hindered by light-scattering in deep-tissue. Hence, BLI is very useful for easy tumor growth measurement during the initial period after tumor cell instillation, but other imaging modalities,

such as high resolution ultrasound, preferably combined with photoacoustic imaging, would be more representative to determine precise tumor volumes as well as the oxygenation of the tissue. However, photoacoustic imaging is not widespread available as compared to BLI measurement. For orthotopic tumor models in general an advice would be to use BLI to determine tumor presence in combination with high resolution ultrasound and photoacoustic imaging to evaluate *in vivo* tumor behavior.

The goal of coupling FimH to Ty21a is to have a safe and immunogenic regimen which reduces the number of instillations required for successful treatment. The orthotopic bladder cancer model is a good model for determining the effect of coupled FimH to Ty21a in NMIBC disease. Our hypothesis was that improved adhesion to the bladder generates a strong antitumor response, as a consequence of prolonged exposure of the the immune system to the pathogen. Despite a significant improved binding of Ty21a+FimH to the bladder wall, a strong additional effect of FimH on mouse survival was not observed in a single *in vivo* study. Only a modest improvement in the median survival of Ty21a+FimH (42,5 days) compared to Ty21a alone (39 days) was revealed. However, improvement of therapy probably requires more than enhanced binding to the bladder wall. The Hbp platform with SpyCatcher/SpyTag system allows in addition to FimH, also the coupling of other proteins that can elicit a desired immune response.

In conclusion, coupling FimH with the Spy-Catcher/SpyTag technology provides an efficient method to decorate Ty21a. Importantly, coupling does not interfere with protein function of FimH or antitumor activity of Ty21a. This method is therefore a promising strategy to optimize antitumor directed responses. The enhanced bacterial binding did not result in significantly better bladder cancer survival *in vivo*, unfortunately. Nevertheless, it would be interesting to analyze the immune responses more extensively to have a better understanding of which responses are required for antitumor activity. The combination of prolonged exposure of the bladder to Ty21a with coupled FimH and/or immunoregulatory target proteins might be the key for the improvement of bladder cancer therapy.

ACKNOWLEDGMENTS

FUNDING

AUTHOR CONTRIBUTIONS

Conception: MJB, LW, JL, WB, CK, CFM; Performance of work: MJB, LW, MV, JM, DH; Interpretation or analysis of data: MJB, LW, CK; Writing the article: LW, MJB, CFM, WB, CK.

CONFLICT OF INTEREST

Maroeska J. Burggraaf, Lisette Waanders, Mariska Verlaan, Janneke Maaskant, Diane Houben, Joen Luirink, Wilbert Bitter, Coen Kuijl and Carla F.M. Molthoff have no conflict of interest to report.

SUPPLEMENTARY MATERIAL

Script for K-Ras analysis (Data 1 and 2). BLI and bladder weight of all mice included in read-out experiment (Data 3). The supplementary material is available in the electronic version of this article: https://dx.doi.org/10.3233/BLC-200382.

REFERENCES

[1] Wu X, Sun T, Medina JJ. In vitro binding of type 1-fimbriated Escherichia coli to uroplakins Ia and Tb: Relation to urinary tract infections. Proc Natl Acad Sci U S A. 1996; 93:9630-35.

[2] Xie B, Zhou G, Chan SY, Shapiro E, Kong XP, Wu XR, Sun TT, Costello CE. Distinct glycan structures of uroplakins Ia and Ib: structural basis for the selective binding of FimH adhesin to uroplakin Ia. J Biol Chem. 2006;281(21): 14644-53.

[3] Berdik C. Unlocking bladder cancer. Nature. 2017;551: S34-35.

[4] Babjuk M, Bohle A, Burger M, Capoun O, Cohen D, Comperat EM, Hernandez V, Kaasinen E, Palou J, Roupret M, van Rhijn BW, Shariat SF, Soukup V, Sylvester RJ, Zigeuner R. EAU Guidelines on Non-Muscle-invasive Urothelial Carcinoma of the Bladder: Update 2016. Eur Urol. 2016;71(3):447-61.

[5] Pettenati C, Ingersoll MA. Mechanisms of BCG immunotherapy and its outlook for bladder cancer. Nat Rev Urol. 2018;15(10):615-25.

[6] Malmstrom PU, Sylvester RJ, Crawford DE, Friedrich M, Krege S, Rintala E, Solsona E, Di Stasi SM, Witjes JA. An individual patient data meta-analysis of the long-term outcome of randomised studies comparing intravesical mitomycin C versus bacillus Calmette-Guerin for non-muscle-invasive bladder cancer. Eur Urol. 2009;56(2): 247-56.

[7] Sylvester RJ, van der Meijden AP, Oosterlinck W, Witjes JA, Bouffioux C, Denis L, Newling DW, Kurth K. Predicting recurrence and progression in individual patients with stage Ta T1 bladder cancer using EORTC risk tables: a combined analysis of 2596 patients from seven EORTC trials. Eur Urol. 2006;49(3):466-5; discussion 75-7.

[8] Domingos-Pereira S, Cesson V, Chevalier MF, Derre L, Jichlinski P, Nardelli-Haefliger D. Preclinical efficacy and safety of the Ty21a vaccine strain for intravesical immunotherapy of non-muscle-invasive bladder cancer. Oncoimmunology. 2017;6(1):e1265720.

[9] Domingos-Pereira S, Sathiyanadan K, La Rosa S, Polak L, Chevalier MF, Martel P, Hojeij R, Derre L, Haefliger JA, Jichlinski P, Nardelli-Haefliger D. Intravesical Ty21a Vaccine Promotes Dendritic Cells and T Cell-Mediated Tumor Regression in the MB49 Bladder Cancer Model. Cancer Immunol Res. 2019;7(4):621-29.

[10] Samuel C, Reddington MH. Secrets of a covalent interaction for biomaterials and biotechnology: SpyTag and Spy-Catcher. Current Opinion in Chemical Biology. 2015(29): 94-99.

[11] van den Berg van Saparoea HB, Houben D, de Jonge MI, Jong WSP, Luirink J. Display of recombinant proteins on bacterial outer membrane vesicles by using protein ligation. Appl Enverion Microbiol. 2018;84:e02567-17.

[12] Zakeri B, Fierer JO, Celik E, Chittock EC, Schwarz-Linek U, Moy VT, Howarth M. Peptide tag forming a rapid covalent bond to a protein, through engineering a bacterial adhesin. Proc Natl Acad Sci U S A. 2012;109(12):E690-7.

[13] Kavoussi LR, Brown EJ, Ritchey JK, Ratliff TL. Fibronectin-mediated Calmette-Guerin bacillus attachment to murine bladder mucosa. Requirement for the expression of an antitumor response. J Clin Invest. 1990;1:62-67.

[14] Iwahi T, Abe Y, Nakao M, Imada A, Tsuchiya K. Role of Type 1 fimbriae in the pathogenesis of ascending urinary tract infection induced by Escherichia coli in mice. Infect Immun. 1983;39(3):1307-15.

[15] Keith BR, Maurer L, Spears A, Orndorff PE. Receptor-Binding Function of Type 1 Pili Effects Bladder Colonization by a Clinical Isolate of Escherichia coli. Infect Immun. 1986;53(3):693-96.

[16] Langermann S, Palaszynski SR, Barnhart M, Auguste G, Pinkner JS, Burlein J, Barren P, Koenig S, Leath S, Jones CH, Hultgren SJ. Prevention of mucosal Escherichia coli infection by FimH-adhesin–based systemic vaccination. Science. 1997;276(5312):607-11.

[17] Connell H, Agace W, Klemm P, Schembri M, Marilds S, Svanborg C. Type 1 fimbrial expression enhances Escherichia coli virulence for the urinary tract. Proc Natl Acad Sci U S A. 1996;93:9827-32.

[18] Scheepbouwer C, Meyer S, Burggraaf MJ, Jose J, Molthoff CF. A Multimodal Imaging Approach for Longitudinal Evaluation of Bladder Tumor Development in an Orthotopic Murine Model. PLoS One. 2016;11(8):e0161284.

[19] Jonathon T Hill BLD, Brent W Bisgrove, Yi-Chu Su, Megan Smith, H Joseph Yost. Poly Peak Parser: Method and Software for Identification of Unknown Indels Using Sanger Sequencing of Polymerase Chain Reaction Products. Developmental Dynamics. 2014;243(12):1632-36.

[20] Li L, Fierer JO, Rapoport TA, Howarth M. Structural analysis and optimization of the covalent association between SpyCatcher and a peptide Tag. J Mol Biol. 2014;426(2): 309-17.

[21] Jong WSP, Daleke-Schermerhorn MH, Vikström D, ten Hagen-Jongman CM, de Punder K, van der Wel N, van de Sandt CE, Rimmelzwaan GF, Follmann F, Agger E, Andersen P, de Gier J, Luirink J. An autotransporter display platform for the development of multivalent recombinant bacterial vector vaccines. Microb Cell Fact. 2014;13(162).

[22] Luo Y, Chen X, Han R, Chorev M, Dewolf WC, O'Donnell MA. Mutated RAS p21 as a target for cancer therapy in mouse transitional cell carcinoma. J Urol. 1999;162(4): 1519-26.

[23] Li R, Sundi D, Zhang J, Kim Y, Sylvester RJ, Spiess PE, Poch MA, Sexton WJ, Black PC, McKiernan JM, Steinberg GD, Kamat AM, Gilbert SM. Systematic Review of the Therapeutic Efficacy of Bladder-preserving Treatments for Non-muscle-invasive Bladder Cancer Following Intravesical Bacillus Calmette-Guerin. Eur Urol. 2020;(78):387-99.

[24] Brausi M, Oddens J, Sylvester R, Bono A, van de Beek C, van Andel G, Gontero P, Turkeri L, Marreaud S, Collette S, Oosterlinck W. Side effects of Bacillus Calmette-Guerin (BCG) in the treatment of intermediate- and high-risk Ta, T1 papillary carcinoma of the bladder: results of the EORTC genito-urinary cancers group randomised phase 3 study comparing one-third dose with full dose and 1 year with 3 years of maintenance BCG. Eur Urol. 2014;65(1):69-76.

[25] Lamm DL, Blumenstein BA, Crissman JD, Montie JE, Gottesman JE, Lowe BA, Sarosdy MF, Bohl RD, Grossman HB, Beck TM, Leimert JT, Crawford ED. Maintenance Bacillus Calmette Guerin Immunotherapy for Recurrent TA, T1 and Carcinoma in sity Transitional Cell Carcinoma of the Bladder: A Randomized Southwest Oncology Group Study. J Urol. 2000;163:1124-29.

[26] Shlomi Tapiero M, Daniel Kedar, Ofer Yossepowitch, Andrei Nadu, Jack Baniel, David Lifshitz, David Margel. Patient Compliance With Maintenance Intravesical Therapy for Nonmuscle Invasive Bladder Cancer. Urology. 2018(118):107-13.

[27] Fiorentino M, Lammers KM, Levine MM, Sztein MB, Fasano A. In vitro Intestinal Mucosal Epithelial Responses to Wild-Type Salmonella Typhi and Attenuated Typhoid Vaccines. Front Immunol. 2013;4:17.

[28] Mulvey MA, Lopez-Boado YS, Wilson CL, Roth R, Parks WC, Heuser J, Hultgren SJ. Induction and evasion of host defenses by Type 1–piliated uropathogenic Escherichia coli. Science. 1998;282:1494-97.